Simulated forward and backward self motion, based on realistic parameters, causes strong motion induced blindness

Victoria Thomas[1*], Matthew Davidson[1], Parisa Zakavi[2], Naotsugu Tsuchiya[1], and Jeroen van Boxtel[1]**

[1]School of Psychological Sciences and Monash Institute of Cognitive and Clinical Neurosciences, Monash University, Clayton 3800 VIC, Australia
[2]Monash Biomedical Imaging, Monash University, Melbourne, Victoria, Australia
[*]victoria.thomas85@gmail.com
[**]j.j.a.vanboxtel@gmail.com

ABSTRACT

Motion Induced Blindness (MIB) is a visual phenomenon whereby highly salient targets disappear when viewed against a moving background mask. While MIB is well established, no research has yet explored whether mask parameters based on patterns of contracting and expanding optic flow can also trigger target disappearance. We aimed to explore MIB using realistic mask speeds that correspond to driving at 35 km/h, 50 km/h, 65 km/h and 80 km/h, as well as simulated forward (expansion) and backward (contraction) motion, 2-D radial movement, random and static mask motion types. Participants (n = 18) viewed MIB targets against masks with different movement types, speed, and target locations. To understand the relationship between small eye movements and perceptual disappearance, we ran two additional experiments with eye tracking (n = 19). Target disappearance increased significantly with faster mask speeds and upper visual field target presentation. Simulated forward and backward motion caused significantly more disappearance than 2-D radial movement, and all moving masks caused significantly more disappearance than a static mask. These effects were not driven by eye-movement differences, suggesting that the realistic optic flow induced by self-motion can cause MIB in an artificial setting. Potential implications for driving safety and Head-Up-Display (HUD) technologies are discussed.

Introduction

Motion Induced Blindness (MIB) is a visual phenomenon whereby highly salient visual targets become temporarily invisible despite their ongoing physical presence in one's visual field, when viewed against the background of a global moving mask (Bonneh,

Cooperman & Sagi, 2001). MIB is one of many bistable perceptual phenomena (Kim & Blake, 2005) used with increasing popularity to investigate the mechanisms of perceptual organisation (Dieter, Tadin & Pearson, 2015; Kloosterman, Meindertsma, Hillebrand, van Dijk, Lamme & Donner, 2015; Libedinsky, Savage & Livingstone, 2009). These bistable phenomena allow subjects to experience varying phenomenology while receiving physically constant visual input, thus, they can help delineate the neural correlates of consciousness by dissociating physical stimuli from conscious perception (Bonneh, Donner, Cooperman, Heeger & Sagi, 2013; Dieter et al, 2015; Kim & Blake, 2005).

MIB has been extensively studied under stimulus parameters designed to optimise perceptual disappearances (Bonneh et al, 2013; Chang, Kanai & Seth, 2015; Wells & Leber, 2014). While it has been suggested that MIB may happen in the real world (e.g., Bonneh, et al, 2001), very little research has aimed to establish this. To date only two predominantly anecdotal studies have explored whether MIB may occur in the real world. Shimojo (2008) used a mirror ball to create a moving mask of bright spots across a room, and was able to cause the perceptual disappearance of a live person in their interactive museum display. Another demonstration of MIB in real life was reported by Inoue, Yagi and Kikuchi (2011), where they induced MIB by superimposing a target over the optic flow of a movie, filmed from the driver's point of view while travelling in a car. Perceptual disappearance was induced much more often while travelling compared to viewing the target over a still frame. Our own pilot studies have also informally replicated this finding, showing that the moving optical flow experienced while driving is able to induce MIB in situations where a stable retinal image is projected to the retina over a moving background. In the current study we aimed to lay the groundwork toward establishing the critical parameters of potential MIB phenomena in much more natural situations, by testing variations of mask speed, trajectory of mask movement and target location based on conditions experienced during real-world self-motion.

The most frequently used display for demonstrating MIB consists of yellow targets and a blue mask of rotating crosses, originally introduced by Bonneh and colleagues (2001). Using this display, various stimulus parameters have been studied (Bonneh et al, 2001; Hsu, Yeh and Kramer, 2004; Metzger, 2009; Mitroff & Scholl, 2005; Sakaguchi, 2006; Schölvinck & Rees, 2009; Shibata, Kawachi & Gyoba, 2010), among which are the effect of target location (Geng, Song, Li, Xu & Zhu, 2007; Nuruki, Oliver, Campana, Wash & Rothwell, 2013; Rosenthal, Davies, Aimola-Davies, & Humphreys; Schölvinck & Rees, 2009; Wells, Leber & Sparrow, 2011; Wallis & Arnold, 2009), mask speed (Bonneh et al, 2001; Grindley & Townsend, 1965; Libedinsky, Savage & Livingstone, 2009), and cues of mask depth (Graf, Adam & Lages, 2002; Rosenthal et al, 2013) on subsequent target disappearance.

In terms of target location, a number of studies have reported greater disappearance when a target is located in the upper left quadrant of the visual display, compared to other tested locations (Bonneh et al, 2001; Bonneh & Donner, 2011; Nuruki et al, 2013;

Rosenthal et al, 2013), or only present targets in the upper left or upper right (Wells et al, 2014; Wells et al, 2011) without a lower field comparison. Bonneh and colleagues (2001) interpreted the top-left bias as the result of processing the global mask at the expense of the local target, mediated by the right-hemisphere dominance of visuospatial attention. A bias towards both upper and left targets has been replicated several times (Bonneh et al, 2001; Bonneh & Donner, 2011; Geng et al, 2007; Grindley & Townsend, 1965; Rosenthal et al, 2013). However, research finding a significant upper left bias generally uses the original three target triangular display (Bonneh et al, 2001), and finds that the bias is greater in relation to the lower central target (Bonneh et al, 2001; Bonneh & Donner, 2011; Nuruki et al, 2013). There has not yet been a controlled comparison of targets presented in all four quadrants of the screen to determine the effects of visual quadrant on disappearance, despite evidence suggesting that upper visual field may exhibit an effect over target disappearance. The trend regarding target location is important to consider when exploring MIB due to its potential relationship with the neural mechanisms of attention (Dieter et al., 2015; Geng et al., 2007). The target location effect is also important when considering the potential for MIB to occur in a driving situation, where the rear-view mirrors tend to be located in upper quadrants and crashes occur more often for cars moving into the left rather than right lane (Road Traffic Authority, 2014; US Department of Transportation, 1994).

It has previously been shown that mask speed influences MIB, with increased speeds leading to both an increased rate and duration of target disappearance (Bonneh et al., 2013; Libidensky et al., 2009). While it has been suggested that it is the temporal frequency rather than retinal speed of the mask underlying MIB (Wallis & Arnold, 2008), trajectory of motion has shown to be equally influential (Wallis & Arnold, 2009). As yet, no study has explored variations in the speed of masks that contract or expand in a way that occurs during simulated self-motion.

Several studies have investigated the effects of other variations in mask composition and movement. In particular, Rosenthal and colleagues (2013) used a three dimensional (3-D) moving mask that mimicked the experience of real world movement and found that significantly more disappearances occurred when masks were perceived to be convex compared to concave, an effect restricted to targets presented in the left field of vision. This and related findings regarding depth ordered masks (Graf et al, 2002), suggests that the 3-D interpretation of the visual scene experienced while driving is likely to influence MIB, providing justification for further research on how depth cues and the optic flow of self-motion influence MIB.

We aim therefore to explore whether mask properties modelled on the real world are conducive to MIB, focussing on mask speeds that would typically occur in a driving situation and the expanding and contracting optic flow experienced in forward and backward self-motion. We also aim to explore the effect of target location on disappearance, to replicate the previously identified upper left bias for disappearance and

to test the hypothesis that MIB is mediated by the right-hemisphere dominant attentional mechanism.

Methods

Participants

Ethics approval was obtained from the Monash University Human Research Ethics Committee, and informed consent was obtained from all participants in the form of written permission prior to participation. Methods were carried out in accordance with the approved guidelines. Thirty-seven participants were recruited at Monash University, all meeting the requirement of normal or corrected-to-normal vision participated in the study. There was no overlap between the 18 participants for Experiment 1 and 3 (aged 18 – 59 years, $M = 24.67$, $SD = 9.42$; 15 females) and 19 participants for Experiment 2 and 4 (aged 18 – 34 years, $M = 23.95$, $SD = 4.30$; 13 females).

Apparatus

All experimental displays were created using Matlab (Mathworks, Natick, MA) and OpenGL, with the PsychToolbox extensions (Brainard, 1997; Pelli, 1997). In Experiments 1 and 3, the experimental display was an IBM P275 CRT powered by a Dell Optiplex9010, and viewed from an approximate distance of 45 cm. In Experiments 2 and 4, the experimental display was a Tobii TX300 powered by a MacBook Pro OS 10.9.5, viewed from an approximate distance of 60 cm. Experiments were run in an experimental room without external lights. Artificial lights were dimmed in Experiment 1 and 3, and were adjusted to a level to provide for proper performance of Tobii TX300 eye tracker in Experiment 2 and 4.

Hereafter, the stimulus specifications presented are for Experiments 1 and 3 with those for Experiments 2 and 4 in brackets. The stimulus consisted of a grey background at 31 Cd/m2 (31 Cd/m2), and white mask dots at 83 Cd/m2 (169 Cd/m2), each with a radius of .05° (.04°). The mask was constructed as a 2-D rendering of a 3-D tunnel with randomly placed dots, through which the participant experienced simulated forward or backward motion. The tunnel was generated anew for each 1-minute trial, had a 5m radius, and was 3000m long. The mask consisted of 7500 white dots, placed randomly on the perimeter of the tunnel. Due to the trial length of 1 minute not all 7500 were seen by the participant. As shown in Supplementary Video S1, dots moved progressively out of a central cluster (about .50° (.38°) radius), at which subjects were instructed to fixate during the experiment. During simulated forward self-motion the speed of dot movement gradually increased as each 'moved nearer' to the participant and approached the periphery of the screen, a pattern which was reversed for backward-motion conditions. Unlike real-life dot progression however, the dots did not change in size with expansion or contraction (Wang, Fukuchi, Koch & Tsuchiya, 2012).

The peripheral perceptual target for MIB was a white disc with an .84° (.63°) radius, surrounded by a thin exclusion boundary of .34° (.25°), through which no mask dots travelled. The disc was located 10.75° (9.32°) degrees diagonal distance from the central fixation cluster, 6.36° (4.61°) vertical and 8.70° (8.10°) horizontal, positioned in either the upper left, upper right, lower left or lower right quadrant of the screen in each trial.

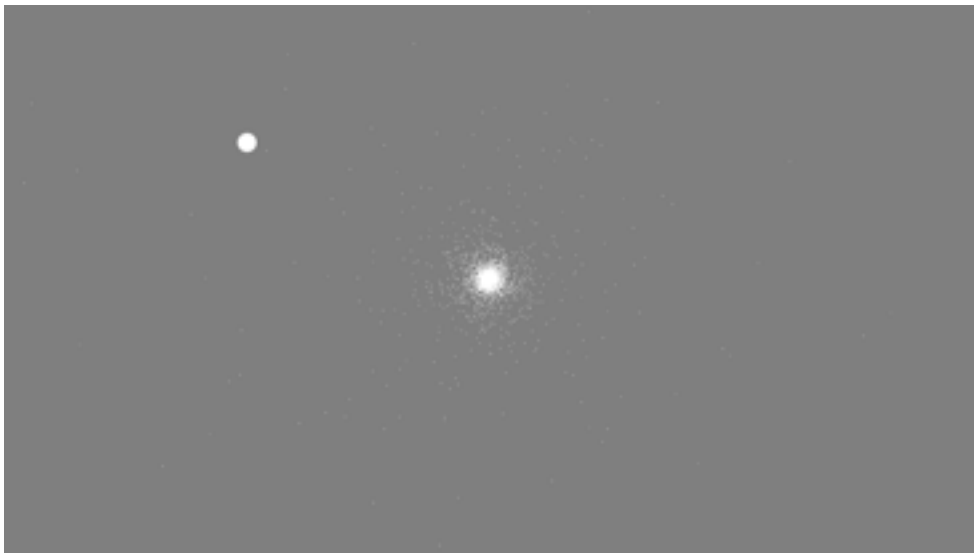

Supplementary Video S1. Experimental display for Experiments 1, 2 and 3

Within each 60-second trial, one catch episode occurred in which the target physically disappeared from the display for a short period of time. The luminance of the target was linearly ramped off over 1.5 seconds, and stayed grey (i.e., the color of the background) for 1-4 seconds, then linearly ramped up to white (i.e., the color of the original target) over another 1.5 seconds. The total duration of the catch episode therefore varied randomly from 4-7 seconds across trials. Each catch episode started between 10s and 50s after the onset of the trial, with its onset time randomly set for every trial. For the subsequent analyses, any reported perceptual disappearance of the target which overlapped with the catch was excluded from analysis. Participants were not told of the catch, but only encouraged to report all perceived disappearances. Accordingly, if the participants did not report physical disappearance of the catch appropriately, we regarded that they had not paid attention to the task in that trial. Debriefing with a number of participants revealed that they were surprised to hear of the catch disappearances, as they had not been able to tell the catch from the genuine perceptual disappearances. While

three participants failed to record the catch on one or more trials, analyses with these participants excluded produced no significant difference to results. Their data was therefore included for analysis.

In Experiments 2 and 4, we also recorded the participants' fixation locations using an eye tracker. Participants had again been instructed to fixate on the central point, and avoid looking directly at the peripheral target at any time. Fixations were defined as any duration between saccades. If the mean fixation duration on the peripheral target per 60-second trial was longer than one second, the participant was considered for exclusion. Only three participants met this exclusion criterion on at least one trial. As including or excluding them did not alter the results in a meaningful way, we included their data for the analyses reported here.

Experiments 1 and 2

Experiments 1 and 2. In Experiments 1 and 2, three different types of mask were presented – expansion (simulated forward motion); contraction (simulated backwards motion), and a static still frame in which there was no dot movement. The simulated movement speed was 65 km/h for both expansion and contraction. The four different target locations were balanced and randomised over trials. Both Experiments 1 and 2 consisted of 12 1-minute trials, presenting each possible combination of mask (3 types) and target location (4 quadrants). Eye-movements were recorded during Experiment 2.

Experiment 3

In Experiment 3, only forward motion was simulated, resulting in an expanding motion pattern. Four different movement speeds were simulated: 35 km/h, 50 km/h, 65 km/h and 80 km/h. Experiment 3 consisted of a total of 16 1-minute trials, presenting each possible combination of speed and target location.

Experiment 4

In Experiment 4, instead of a central cluster, the fixation point was explicitly presented as a white cross with a size of 0.50° x 0.50° (Supplementary Video S2). The cross was surrounded by an exclusion radius of 2.35°, through which no mask dots travelled. In addition, only in Experiment 4, dots (500 in total) moved at a constant speed of 3.4° per second. Four different types of mask were presented: 2-D radial expansion, 2-D radial contraction, 2-D static and 2-D random movement. With the random type of mask movement, the dots moved in a random direction and had a 1% chance of being removed on each frame. Removed dots, and dots which crossed the outer edge of the display were replaced at a random position on the screen. Experiment 4 consisted of 16 1-minute trials, presenting each possible combination mask type and target location. Due to the stimulus layout, this experiment had a uniform distribution of mask dots on the screen, while the other experiments had a decreasing density with increasing eccentricity.

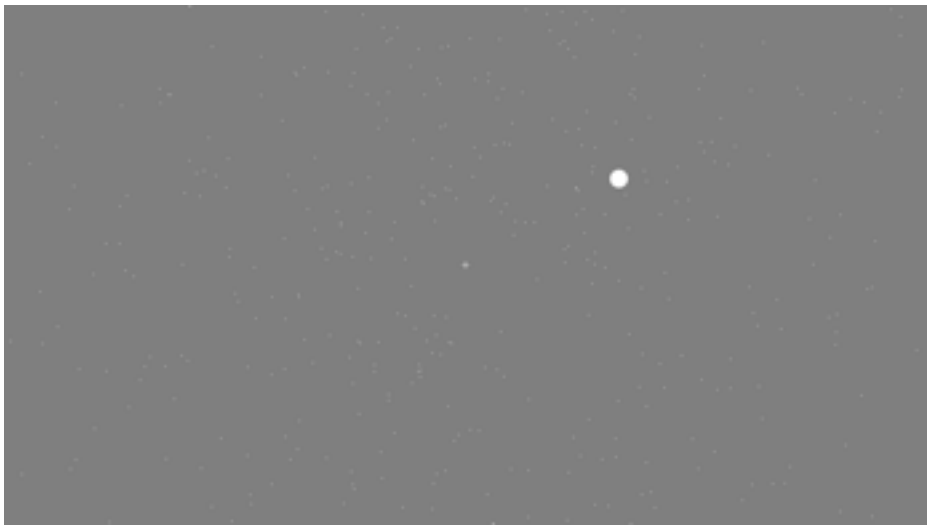

Supplementary Video S2. Experiment 4 stable mask speed display

Procedure

Experiments 1 and 3

Participants sat comfortably in front of the computer, with their head stabilised by a chin rest. They were instructed to fixate on the central area of the screen and to indicate the perceptual invisibility of the target by holding down the spacebar for as long as the target remained invisible while paying attention to the peripheral target, without looking at it directly.

Experiments 2 and 4

Experiments 2 and 4 followed the same procedure as 1 and 3, however eye movements were also recorded. Participants underwent a standard 9-point eye-tracking calibration before the experiment started, and did not move their heads away from the chin rest for the duration of the experiment.

Eye movements were recorded binocularly using a Tobii TX-300 Eyetracker (Tobii Technology, Danderyd, Sweden) at a sampling rate of 300Hz, controlled through the software package T2T (http://psy.cns.sissa.it/t2t/About T2T.html). Saccades and fixations were detected offline using a velocity-based algorithm (Engbert & Kliegl, 2003). Saccades with the amplitude larger or less than 1 degree of visual angle were categorised as macro-saccades or micro-saccades, respectively.

Analyses

We ran two repeated measures ANOVAs for each experiment. The mean duration of target disappearance per condition was the dependent variable (DV). The first analysis was a one-way ANOVA with mask condition as the sole independent variable (IV). The second was a two-way ANOVA, with upper versus lower and left versus right target presentation as the two IVs. The same analyses were also run for the mean rate of target disappearance per condition, and the results were nearly identical to those for the mean duration of disappearance. Therefore, to avoid repetition only the results for mean duration are reported. Assumptions for all tests were met, with the exception of violated normality in several conditions across experiments. Therefore, unless otherwise stated a square root data transformation was performed for all experiments, as small sample size (<30) meant the Central Limit Theorem was not applicable in correcting normality (Field, 2012; Tabachnick & Fidell, 2013; Hair, Black, Babin & Anderson, 2009). A constant of 1 was added to all data when performing the transformation, due to the dataset containing 0 values (Field, 2012). Despite the transformation, normality was occasionally still violated in the static mask condition across Experiments 1, 2 and 4, with skewness Z-Scores exceeding the alpha =.05 cutoff of 1.96 (Field, 2012; Tabachnick & Fidell, 2013). Alternate transformations (Log10, Reciprocal) also failed to correct normality in this variable. The violation in the static mask control condition was due to the majority of participants recording disappearance scores of zero for this condition, as expected. Given that negative values were not possible in our study, this necessarily led to a skewed distribution in the static condition. As the violated static condition was serving as a control for comparison only, the square root transformation was retained and tests run despite the violation. However, non-parametric Friedman's tests corroborated our findings in all cases. All graphical representations of data were created using within-subjects error bars displaying a 95% confidence interval, as recommended by Cousineau (2005). In all figures, double asterisks (**) indicate significance at a <.01 level, and a single asterisk (*) indicates significance at a <.05 level.

Results

MIB can be induced by the optic flow of simulated forward and backward self-motion

The design of Experiments 1 and 2 were identical in all aspects, with the exception of the use of an eye-tracking device in Experiment 2 to monitor eye movements (as well as a small variation in viewing distance, see Method). There was a significant main effect of mask type on mean duration of target disappearance in both Experiment 1 ($F(2, 32) = 21.02$, $p < .001$) and Experiment 2 ($F(2, 36) = 39.94$, $p < .001$). Pairwise comparisons for Experiment 1 (Figure 1) revealed that target disappearance in the static control condition was significantly shorter than during both expansion ($F(1, 16) = 25.84$, $p < .001$, $r = .79$) and contraction ($F(1, 16) = 29.10$, $p < .001$, $r = .80$). This was replicated in Experiment 2 (Figure 2), which also found static target disappearance to be significantly shorter than during both expansion ($F(1, 18) = 43.50$, $p < .001$, $r = .84$), and contraction ($F(1, 18) =$

56.31, p <.001, r = .87). In both experiments, expansion and contraction were not significantly different from each other (p >.05).

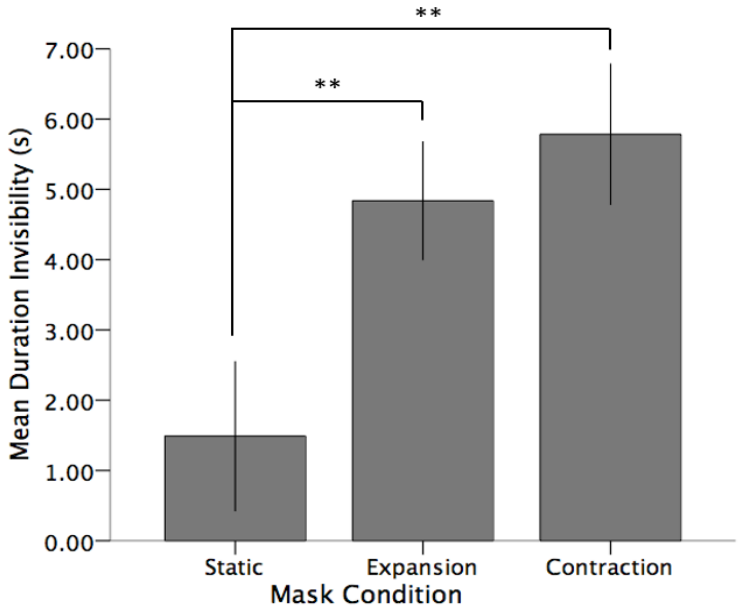

Figure 1. Mean duration of target disappearance dependent on movement type within Experiment 1

Eye-tracking analyses

Eye-tracking data from Experiment 2 showed that mean number of macro-saccades was also significantly affected by the type of mask ($F(2, 36) = 8.09$, $p = .001$). Pairwise comparisons indicated that in Experiment 2 the static condition had significantly more macro-saccades than expansion ($F(1, 18) = 7.91$, $p = .012$, $r = .55$) and contraction ($F(1, 18) = 10.50$, $p = .005$, $r = .61$). However, there was no significant difference between expansion and contraction motion types (p >.05; Figure 2).

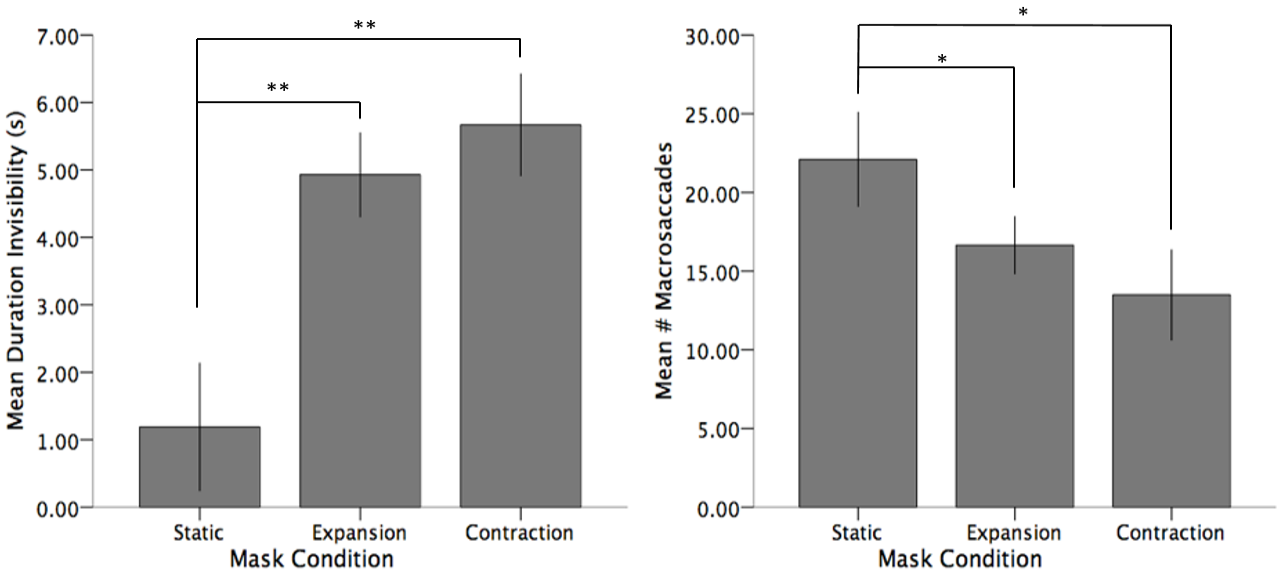

Figure 2. Mean duration of target disappearance (left panel) and mean number of macro-saccades (right panel), dependent on movement type within Experiment 2.

When comparing the two plots in Figure 2, target disappearance appears to be negatively correlated with an increased number of macro-saccades. To ensure that the significant result of target disappearance between mask conditions was not solely a result of the corresponding significant variation in saccades, we plotted the mean duration of MIB against the mean number of macro-saccades (>1 deg, Figure 3, left panel) or macro+micro-saccades (<1 deg, right panel) for all three conditions, to compare the effect separately within conditions. As can be seen in Figure 3, the trend for target disappearance to decrease as saccades increased was found separately for expansion and contraction mask conditions. Importantly, the presence of micro and macro-saccades did not completely explain the lower occurrence of MIB in the static condition, as the mean target disappearance fell below expansion and contraction over the entire range of saccade frequency. Further regression analysis revealed that the 95% confidence intervals of the y-intercepts of both the contraction and expansion data did not overlap with the 95% confidence interval of the static data, strongly suggesting that the eye-movements did not cause the difference between the conditions.

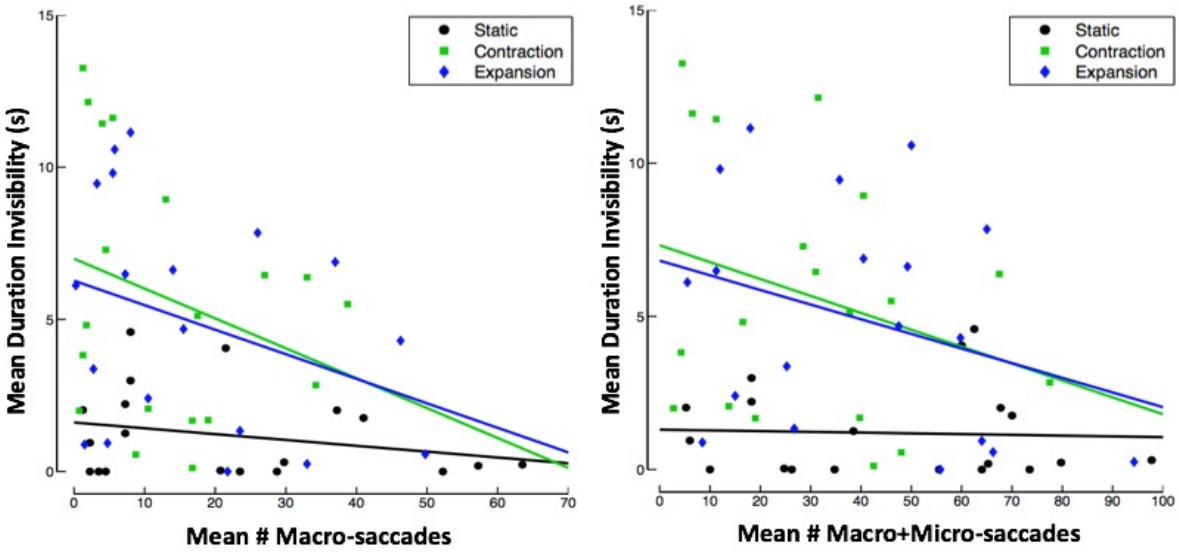

Figure 3. Relationship between mean number of macro and macro+micro saccades and target disappearance per minute within each mask condition of Experiment 2

MIB is dependent on the speed of simulated self forward motion

In Experiment 3, we examined the effects of the simulated speed of self forward motion. There was a significant main effect of speed on target disappearance ($F(3, 51) = 5.97$, $p = .001$) as seen in Figure 4. Pairwise comparisons revealed that disappearances for the lowest speed level of 35km/h were significantly shorter than 50km/h ($F(1, 17) = 6.84$, $p = .018.$, $r = .54$), 65 km/h ($F(1, 17) = 17.09$, $p <.001.$, $r = .71$), and 80 km/h ($F(1, 17) = 11.68$, $p = .003.$, $r = .64$). Polynomial contrasts also indicated a significant positive linear trend of target disappearance across conditions ($F(1, 17) = 14.09$, $p = .002$, $r = .67$).

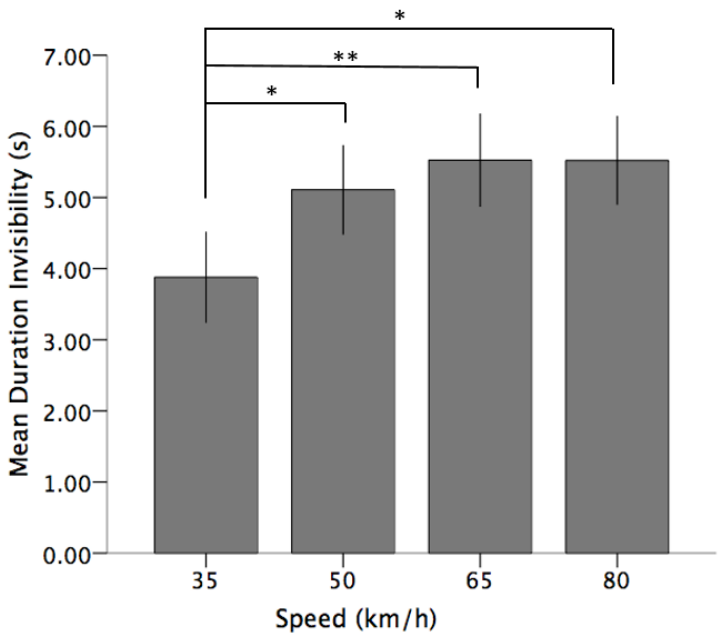

Figure 4. Mean duration of target disappearance for each mask speed condition within Experiment 3

MIB due to static, random and radial mask motion at a constant dot speed

Finally, Experiment 4 looked at target location and the direction of mask movement during 2-D radial movement in which dot speed was held constant across the screen, unlike the simulated self-motion in Experiments 1, 2 and 3. There was a significant main effect of the direction of mask movement on target disappearance ($F(3, 54) = 18.23$, p ¡ .001; Figure 5). Pairwise comparisons revealed that the static control condition had a significantly lower mean duration of disappearance than during 2-D random ($F(1, 18) = 27.80$, $p < .001$, $r = .78$), 2-D radial expansion ($F(1, 18) = 24.11$, $p < .001$, $r = .76$) and 2-D radial contraction conditions ($F(1, 18) = 22.10$, $p < .001$, $r = .74$). However, 2-D random, 2-D radial expansion and 2-D radial contraction were not significantly different from each other ($p > .05$).

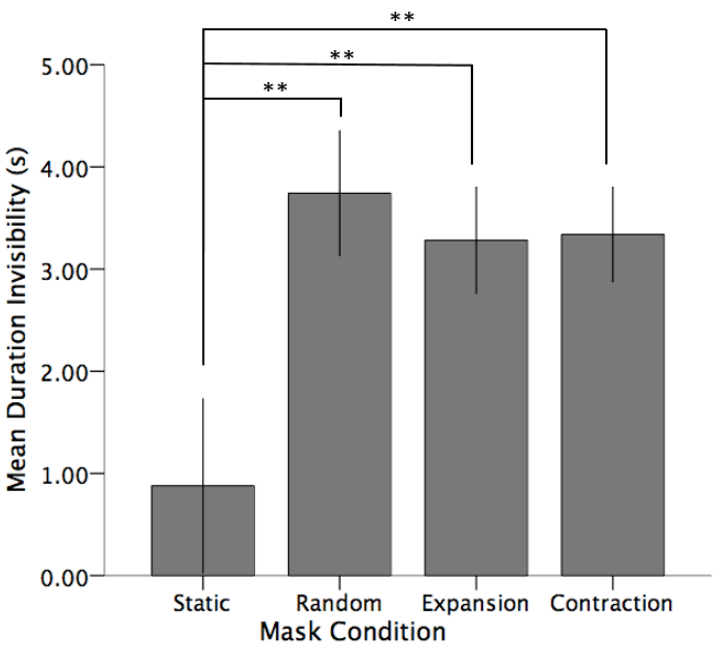

Figure 5. Mean duration of target invisibility dependent on motion type in Experiment 4

Interestingly, target disappearance was found to be significantly different between Experiment 2 (simulated forward and backward motion) and Experiment 4 (2-D radial movement; $F(4, 72) = 14.36$, $p < .001$; see Figure 6). Importantly, the same participants participated Experiment 2 and 4 and thus this difference cannot be explained by the individual differences. Simulated forward motion induced significantly longer target disappearances than 2-D radial expansion ($F(1, 18) = 13.15$, $p = .002$, $r = .65$), 2-D radial contraction ($F(1, 18) = 16.04$, $p < .001$, $r = .69$) and 2-D random movement ($F(1, 18) = 10.14$, $p = .005$, $r = .60$). Likewise, simulated backward motion also induced significantly longer target disappearances than 2-D radial expansion ($F(1, 18) = 31.93$, $p < .001$, $r = .80$), 2-D radial contraction ($F(1, 18) = 30.38$, $p < .001$, $r = .79$) and 2-D random movement ($F(1, 18) = 30.90$, $p < .001$, r = .79).

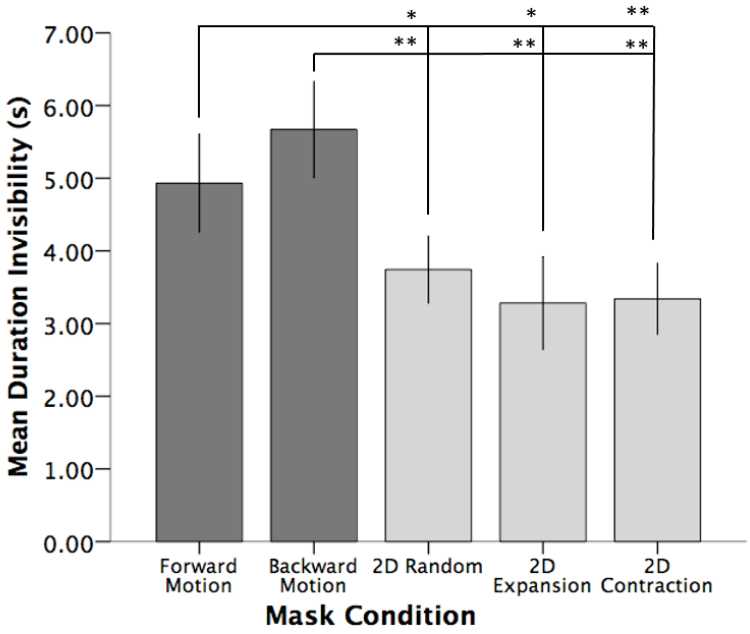

Figure 6. Mean duration of target invisibility across mask conditions of Experiments 2 (dark bars) and 4 (light bars). Note that the participants for Experiment 2 and 4 were identical

However, dot speeds around the target were quite different in Experiment 3, depending on simulated forward motion. Therefore, we also compared the data of Experiment 4 to the 35 km/h condition of experiment 3, which had a mask speed of 3.8° per second around the target. This closely matched the 3.4° of movement per second within Experiment 4. In this comparison no significant difference in MIB between conditions was found (all $p<.05$).

Eye-tracking analyses

In Experiment 4, the number of saccades did not differ significantly across conditions (data not shown).

Effects of Target Location in MIB

In the previous analyses we did not include target location as an independent variable, because it proved impossible to meet the assumption of normality (see Methods) to perform two-way ANOVAs in that case. Therefore, we decided to analyse target location using separate two-way ANOVAs for each experiment, with independent variables being

upper versus lower visual field, and left versus right visual field. Experiment 2 was the only experiment which showed a significant main effect, with target disappearance in the upper visual field being significantly longer than the lower visual field ($F(1, 18) = 45.20$, $p < .001$). Neither the main effect for left versus right visual field or the interaction effect was significant ($p > .05$).

When target location data from all four experiments was collated (Figure 7), a two-way ANOVA again found that significantly more disappearance occurred for targets in the upper compared to lower visual field ($F(1, 72) = 17.00$, $p < .001$). There was no significant main effect of target presentations between the left and right fields of vision. Interaction was also not significant ($p > .05$).

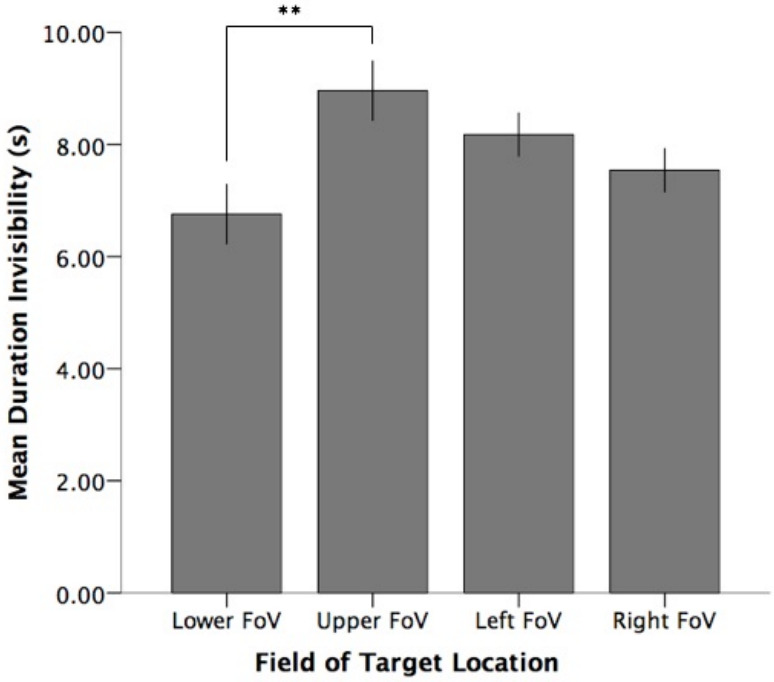

Figure 7. Mean duration of invisibility according to target visual field across all experiments

When replotting the data according to individual quadrant (Figure 8), we can see that target disappearance was greatest in the upper left quadrant compared to all others. Pairwise comparisons revealed that target disappearance in the lower left condition was significantly lower than during both upper left ($F(1, 18) = 24.97$, $p < .001$, $r = .76$) and upper right target presentations ($F(1, 18) = 18.44$, $p < .001$, $r = .71$). Likewise, target

disappearance in the lower right condition was significantly lower than during both upper left ($F(1, 18) = 30.48, p < .001, r = .79$) and upper right target presentations ($F(1, 18) = 16.40, p = .001, r = .69$). Both lower left and lower right, and upper left and upper right target presentations were not significantly different from each other.

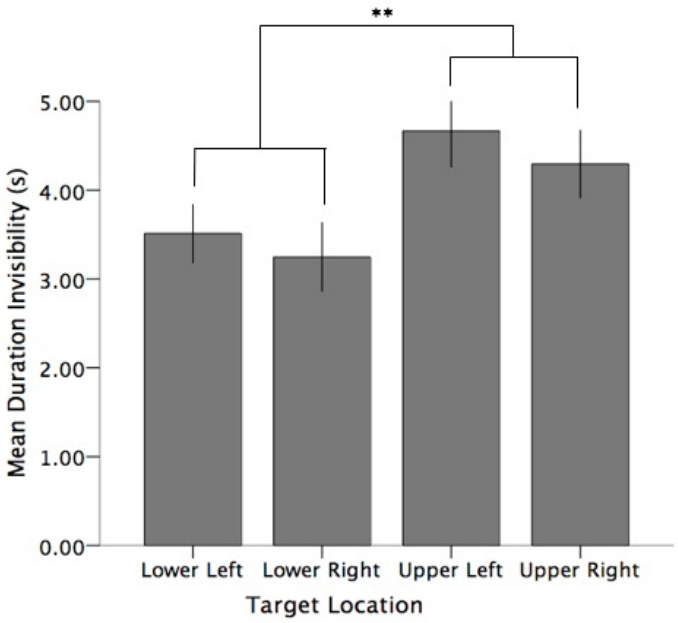

Figure 8. Mean duration of invisibility according to target quadrant across all experiments

Discussion

In the current study we tested whether display parameters modelled on optic flow simulating self-motion are able to induce MIB. Various other motion patterns have been used in the past (Bonneh et al, 2001; Rosenthal et al, 2013; Wallis & Arnold, 2009; Wells et al, 2011), but none have used a contracting or expanding optic flow analogous to when walking or driving, despite cues of self-motion being essential to safe navigation in altering environments (Britten, 2008). The present study showed that optic flow patterns similar to those experienced when driving a car in a realistic speed range can reliably elicit MIB.

Mask Speed

We found that mean duration of target disappearance increased with mask speed, consistent with previous research (Bonneh et al, 2001; Libedinsky et al, 2009). Specifically, our three upper mask speeds of 50km/h, 65km/h and 80km/h elicited significantly longer disappearances than the lowest of 35km/h. There was no significant difference found between the three upper speeds, suggesting that there may be a limit to increased target disappearance that is reached between 35 – 50 km/h. Further research is needed with a wider range of speeds to establish whether an 'optimal' range of mask speed for inducing target disappearance exists, and where the upper threshold of it might be. Our findings regarding mask speed may hold implications for driving safety, as it is known that driving speed is significantly related to accident rates (Road Traffic Authority, 2012; 2014). Given that the speed of the mask is also significantly related to target disappearance, it is possible that MIB disappearance occurring in the real world plays a role in traffic accidents at certain speeds where stationary targets (such as rear view mirror or windscreen-mounted GPS devices) are viewed over the moving landscape.

Mask Movement

While mask movement was conducive to target disappearance, disappearance was not affected by variations in the direction of movement that we tested within each experiment, with optic flow expansion and contraction causing comparable target disappearance. However, when comparing across experiments it was found that expanding and contracting optic flow simulating self-motion (i.e., increasing speeds at increased eccentricity) caused significantly longer (and more frequent) target disappearance compared to that induced by 2-D radially expanding, contracting, and random movement at one constant speed. While a follow up analysis found that the effect may have been a result of greater mask speed around the target rather than the type of movement itself, the finding is still interesting, particularly when considering the potential role of dot density. Simulated forward and backward motion mask patterns naturally decrease in dot density at larger eccentricities, in contrast to the 2-D radial expansion and contraction, which maintain the same density across the display at any time. While expanding and contracting optic flow did display greater mask speed around the target, they also had around a 9-times lower dot density at target eccentricity. Lower mask density necessarily results in less competition between the mask and target, causing less target disappearance (Wells et al, 2011). Therefore, it is possible that an even stronger disappearance effect within simulated forward and backward motion could have been observed if we were to equate dot density around the target in these conditions. Further research addressing inconsistencies in mask movement and dot density around the target will be needed to explore this possibility.

Target Location

We found significantly longer target disappearance for upper visual field presentation compared to lower visual field. Consistent with previous research (Bonneh et al, 2001; Rosenthal et al, 2013; Geng et al, 2007), there was a trend for target disappearance to be

greatest for presentations in the upper left quadrant of the screen, and higher in the left visual field overall compared to the right, although these we not significant effects. Past research has taken the increased disappearance of upper left targets to suggest a possible neural mechanism underlying MIB (Bonneh et al, 2001), such as spatial attention, which also shows strong visual field asymmetry (Mondor & Bryden, 1992; Rhodes & Robertson, 2002). However, most studies that report such a bias presented three targets in a triangular display with two targets in the upper field and one in the lower field. Significant results were found only between the upper left and lower central target (Bonneh et al, 2001; Bonneh & Donner, 2011; Nuruki et al, 2013). If we interpret this in light of our current findings, it is possible that the upper left bias in MIB builds largely on a strong bias to the upper field overall.

The upper field bias of perceptual disappearance is compatible with research which suggests greater visual acuity for the lower visual field (He, Cavanagh & Intriligator 1996), where object recognition in natural scenes is particularly important for our self-motion, hunting and general survival (He et al, 1996; 1997). The greater advantage in the lower visual field has been reported in a number of visual tasks: target detection and discrimination (Levine & McAnany, 2005), visual acuity and contrast sensitivity (Fuller, Rodriguez, & Carrasco, 2008; Skrandies, 1987), and perception of illusory contours (Rubin, Nakayama, & Shapley, 1996). This may explain the trend for less target disappearance in the lower visual field, as a consequence of greater visual acuity.

Saccades and the link to driving

The results of our eye-tracking data showed that target disappearance decreased as either macro or the total number of saccades increased within each mask movement condition, a finding consistent with previous research (Bonneh et al, 2011; Hsieh & Tse, 2009). This relationship between saccades and target disappearance was found within the moving mask conditions separately, but not the static condition. However, eye-movements did not eliminate MIB, which is consistent with an observation that MIB occurs even with a moving target (Bonneh et al, 2001).

There was a mean number of 16.64 macro-saccades per minute during the expansive optic flow mask condition, and 13.50 macro-saccades per minute in the contractive condition. While around 83 macro-saccades per minute typically occur while driving - a value much higher than found in our experiments - there is great variation in this according to the type of road and environment (Chapman & Underwood, 1998). Fewer saccades and longer fixations occur on rural as opposed to urban roads (Chapman & Underwood, 1998; Underwood, Crundall & Chapman, 1997), where fatality rates are also consistently higher (Road Traffic Authority, 2012; 2014). While the frequency of saccades in our experiments were relatively low across subjects, there were some subjects who exhibited 30-40 macro-saccades or 50-70 micro-saccades per minute (Figure 3) and still reported substantial durations of target disappearance (~5 sec per minute). This suggests that MIB is likely to occur in the real world. Assuming that 5 seconds of MIB

can occur per minute for the saccade rates reported herein, then up to 10 minutes of potentially fatal MIB may occur during a two-hour drive.

Limitations and Implications

Collectively, our findings suggest that MIB is likely to occur in the real world. Most importantly, we have shown that the optic flow simulating rapid self-movement successfully elicits MIB. The potential for MIB to occur in the world may hold strong implications for driving safety, where the most common point of gaze is at the centre of the expansion point of the approaching road (Helander & Söderberg, 1972; Mourant & Rockwell, 1997; Shinar, McDowell & Rockwell, 1977), while items that need to be monitored reside in upper visual quadrants which are prone to target disappearance. It has also been suggested that fixations lengthen and saccade frequency decreases during times of danger or hazard (Chapman & Underwood, 1998), when multi-tasking (May, Kennedy, Williams, Dunlap & Brannan, 1990; Reimer, 2009) and when we experience fatigue (Di Stasi, McCamy, Catena, Macknik & Cañas, 2013). Given that fewer saccades correlate with greater target disappearance, MIB may be more likely to occur during hazardous situations, or driver fatigue - which is also the second highest influencing factor in traffic accidents in NSW Australia, behind only alcohol consumption (Road Traffic Authority, 2015). A potential critical target for disappearance during driving is the stationary rear-view mirror, which is positioned in the upper field. Although the visual objects in the mirror are not stationary, MIB is known to occur for targets that move, flicker and even change colour (Bonneh et al., 2001; Chang, Kanai & Seth, 2015). Future research should ascertain whether the entire mirror or the visual objects within are subject to MIB, to understand the potential causes of rear-end accidents.

MIB in the real world may also hold implications for the development of Head-Up Display (HUD) technology, where crucial information is projected onto the screen in the form of stable symbols and text, through which the moving background of road or land is viewed. Such technology can be found, for example, in the use of F-35 Fighter Jet helmets which have been developed to project flight information onto the visor viewed by the pilot over the moving background (The F-35 Helmet, 2015), or increasingly in commercially available cars with dashboard information projected onto the windscreen (Hyundai Future Transport Technology, 2015). Given MIB is remarkably robust under normal viewing conditions, and is induced more strongly by the optic flow expansion and contraction that would be experienced in driving, flying and walking, further research is warranted to ascertain its significance in relation to these new technologies.

While providing support for the occurrence of MIB in the natural world, it must be noted that our research was still undertaken in an artificial setting. The experiment was conducted on a computer display, and while parameters were modelled on the real world, aspects of the display itself were also inconsistent with the type of motion perceived in daily life. Specifically, the mask dots did not increase in size as they approached the

periphery, as would occur in normal optic flow movement (Wang et al, 2012). Additionally, the mask was based on a tunnel, yet driving through tunnels in reality is usually brief and infrequently experienced. Future research should attempt to measure the occurrence of MIB directly in conditions that approximate the statistics of the real world experience in a closer fashion, especially given its potential impact on driving safety.

Author contributions statement

VT and JVB conceptualised and designed the research reported in this article, with feedback from NT and MD. VT collected and analysed the behavioural data, with help from JVB. VT wrote the article, with feedback from JVB, MD and NT. MD programmed the experiments, with help from JVB. PZ analysed the eye-movement data.

Additional information

Competing financial interests

The authors declare no competing financial interests.

References

Britten, K. H. (2008). Mechanisms of Self-Motion Perception. *Annual Review of Neuroscience, 31,* 389-410. Doi: 10.1146/annurev.neuro.29.051605.112953

Bonneh, Y. S., Cooperman, A., & Sagi, D. (2001). Motion-induced blindness in normal observers. *Nature*, *411*(6839), 798–801. Doi: http://doi.org/10.1038/35081073

Bonneh, Y. S., & Donner, T. H. (2011). Motion-induced Blindness. *Scholarpedia, 6*(6). Doi: 10.4249/scholarpedia.3321

Bonneh, Y. S., Donner, T. H., Cooperman, A., Heeger, D. J., & Sagi, D. (2013). Motion-induced Blindness and Troxler Fading: Common and Different Mechanisms. *PLoS ONE, 9*(3). Doi: http://doi.org/10.1371/journal.pone.0092894

Bonneh, Y. S., Donner, T. H., Sagi, D., Fried, M., Heeger, D. J., & Arieli, A. (2011). MIB and microsaccades: cause and effect. *Journal of Vision 10*(14). Doi: http://doi.org/10.1167/10.14.22.

Brainard, D. H. (1997). The Psychophysics Toolbox. *Spatial Vision*, *10*(4), 433–436. Doi: http://doi.org/10.1163/156856897X00357

Centre for Road Safety, Transport for NSW. (2012). *Road Traffic Crashes in NSW: Statistical Statement for the year ended 31 Dec 2012.* Retrieved from http://roadsafety.transport.nsw.gov.au/downloads/crashstats2012.pdf

Centre for Road Safety, Transport for NSW. (2014). *Road Traffic Crashes in NSW: Statistical Statement for the year ended 31 Dec 2014.* Retrieved from http://roadsafety.transport.nsw.gov.au/downloads/crashstats2014.pdf

Centre for Road Safety, Transport for NSW. (2015). *NSW Crash Data.* Retrieved from http://roadsafety.transport.nsw.gov.au/statistics/interactivecrashstats/nsw.html?tabnsw=3

Chang, A. Y. C., Kanai, R., & Seth, A. K. (2015). Cross-modal prediction changes the timing of conscious access during the motion-induced blindness. *Consciousness and Cognition*, *31*, 139–147. Doi: http://doi.org/10.1016/j.concog.2014.11.005

Chapman, P. R., & Underwood, G. (1998). Visual search of driving situations: Danger and experience. *Perception*, *27*, 951–964. Retrieved from http://www.psychology.nottingham.ac.uk/staff/gju/underwood_papers/Perception.1998.pdf

Cousineau, D. (2005). Confidence intervals in within-subject designs: A simpler solution to Loftus and Masson's method. *Tutorials in Quantitative Methods for Psychology*, *1*(1), 42–45. Retrieved from http://doe.concordia.ca/CSLP/Downloads/PDF/Confidence%20intervals..art.pdf

Di Stasi, L. L., McCamy, M. B., Catena, A., Macknik, S. L., Cañas, J. J., & Martinez-Conde, S. (2013). Microsaccade and drift dynamics reflect mental fatigue. *European Journal of Neuroscience*, *38*(3), 2389–2398. Doi: http://doi.org/10.1111/ejn.12248

Dieter, K. C., Tadin, D., & Pearson, J. (2015). Motion-induced blindness continues outside visual awareness and without attention. *Scientific Reports*, *5*(11841), 1–8. Doi: http://doi.org/10.1038/srep11841

Engbert, R., & Kliegl, R. (2003). Microsaccades uncover the orientation of covert attention. *Vision Research, 43*99), 1035-1045. Doi: 10.1016/S0042-6989(03)00084-1

Field, A. (2012). *Discovering Statistics Using IBM SPSS Statistics* (4th ed.). London: SAGE Publications Ltd

Fuller, S., Rodriguez, R. Z., & Carrasco, M. (2008). Apparent contrast differs across the vertical meridian: visual and attentional factors. *Journal of Vision*, *8*(1), 1–16. Doi: http://doi.org/10.1167/8.1.16

Geng, H., Song, Q., Li, Y., Xu, S., & Zhu, Y. (2007). Attentional modulation of motion-induced blindness. *Chinese Science Bulletin*, *52*(8), 1063–1070. Doi: http://doi.org/10.1007/s11434-007-0178-0

Graf, E. W., Adams, W. J., & Lages, M. (2002). Modulating motion-induced blindness with depth ordering and surface completion. *Vision Research*, *42*(25), 2731–2735. Doi: http://doi.org/10.1016/S0042-6989(02)00390-5

Grindley, G. C., & Townsend, V. (1965). Binocular masking induced by a moving object. *Quarterly Journal of Experimental Psychology*, *17*(2), 97–109. Doi: http://doi.org/10.1080/17470216508416418

Hair, J. F., Black, W. C., Babin, B. J. & Anderson, R. E. (2014). *Multivariate Data Analysis* (7th ed.). Essex: Pearson Education Limited.

He, S., Cavanagh, P., & Intriligator, J. (1996). Attentional resolution and the locus of visual awareness. *Nature*, *383*(6598), 334-337. Doi: http://doi.org/10.1038/383334a0

He, S., Cavanagh, P., & Intriligator, J. (1997). Attentional resolution. *Trends in Cognitive Sciences*, *1*(3), 115–121. Doi: http://doi.org/10.1016/S1364-6613(97)89058-4

Helander, M., & Söderberg, S. (1972). *Driver Visual Behavior and Electrodermal Response During Highway Driving.* Göteborg, Sweden: University of Göteborg. Retrieved from https://books.google.com.my/books?id=ZSYecgAACAAJ

Hsieh, P. J., & Tse, P. U. (2009). Microsaccade rate varies with subjective visibility during motion-induced blindness. *PLoS ONE*, *4*(4), 1–9. Doi: http://doi.org/10.1371/journal.pone.0005163

Hsu, L. C., Yeh, S. L., & Kramer, P. (2004). Linking motion-induced blindness to perceptual filling-in. *Vision Research*, *44*(24), 2857–2866. Doi: http://doi.org/10.1016/j.visres.2003.10.029

Hyundai Future Transport Technology. (n.d.). Retrieved on September 1 2015, from http://www.hyundai.com.au/hyundai-info/news/2015/01/hyundai-showcase-technology-at-ces

Inoue, K., Yagi, Y., & Kikuchi, T. (2011). Perceptual Disappearance of a Visual Object in a Driving Situation. *Psychologia, 54*(2), 87–95. Doi: http://doi.org/10.2117/psysoc.2011.87

Kim, C. Y., & Blake, R. (2005). Psychophysical magic: rendering the visible 'invisible'. *Trends in Cognitive Sciences*, *9*(8), 381–388. Doi: http://doi.org/10.1016/j.tics.2005.06.012

Kloosterman, N. A., Meindertsma, T., Hillebrand, A., van Dijk, B. W., Lamme, V. A. F., & Donner, T. H. (2015). Top-down modulation in human visual cortex predicts the stability of a perceptual illusion. *Journal of Neurophysiology, 113*, 1063–1076. Doi: 10.1152/jn.00338.2014

Levine, M. W., & McAnany, J. J. (2005). The relative capabilities of the upper and lower visual hemifields. *Vision Research*, *45*(21), 2820–30. Doi: http://doi.org/10.1016/j.visres.2005.04.001

Libedinsky, C., Savage, T., & Livingstone, M. (2009). Perceptual and physiological evidence for a role for early visual areas in motion-induced blindness. *Journal of Vision*, *9*(1), 1–10. Doi: http://doi.org/10.1167/9.1.14.Introduction

May, J. G., Kennedy, R. S., Williams, M. C., Dunlap, W. P., & Brannan, J. R. (1990). Eye movement indices of mental workload. *Acta Psychologica*, *75*(1), 75–89. Doi: http://doi.org/10.1016/0001-6918(90)90067-P

Metzger, W. (2006). *Laws of Seeing*. Cambridge: MIT Press

Mitroff, S. R., & Scholl, B. J. (2005). Forming and updating object representations without awareness: evidence from motion-induced blindness. *Vision Research*, *45*(8), 961–967. Doi: http://doi.org/10.1016/j.visres.2004.09.044

Rhodes, D. L., & Robertson, L. C. (2002). Visual field asymmetries and allocation of attention in visual scenes. *Brain and Cognition*, *50*(1), 95–115. http://doi.org/10.1016/S0278-2626(02)00014-3

Mourant, R. R., & Rockwell, T. H. (1970). Mapping eye-movement patterns to the visual scene in driving: An exploratory study. *Human Factors*, *12*(1), 81–87. Doi: http://doi.org/10.1177/001872087001200112

Nuruki, A., Oliver, R., Campana, G., Walsh, V., & Rothwell, J. C. (2013). Opposing roles of sensory and parietal cortices in awareness in a bistable motion illusion. *Neuropsychologia*, *51*(13), 2479–2484. Doi: http://doi.org/10.1016/j.neuropsychologia.2013.09.026

Pelli, D. G. (1997). The VideoToolbox software for visual psychophysics: transforming numbers into movies. *Spatial Vision*, *10*(4), 437–442. Doi: http://doi.org/10.1163/156856897X00366

Reimer, B. (2009). Impact of Cognitive Task Complexity on Drivers' Visual Tunneling. *Transportation Research Record: Journal of the Transportation Research Board*, *2138*, 13–19. Doi: http://doi.org/10.3141/2138-03

Rhodes, D. L., & Robertson, L. C. (2002). Visual field asymmetries and allocation of attention in visual scenes. *Brain and Cognition*, *50*(1), 95–115. Doi: http://doi.org/10.1016/S0278-2626(02)00014-3

Rubin, N., Nakayama, K., & Shapley, R. (1996). Enhanced Perception of Illusory Contours in the Lower Versus Upper Visual Hemifields. *Science*, *271*(5249), 651–653. Doi: http://doi.org/10.1126/science.271.5249.651

Rosenthal, O., Davies, M., Aimola-Davies, A. M., & Humphreys, G. W. (2013). A role of 3-D surface-from-motion cues in motion-induced blindness. *Perception*, *42*(12), 1353–1361. Doi: http://doi.org/10.1068/p7560

Sakaguchi, Y. (2006). Contrast dependency in perceptual filling-in. *Vision Research*, *46*(20), 3304–12. Doi: http://doi.org/10.1016/j.visres.2006.05.015

Schölvinck, M. L., & Rees, G. (2009). Attentional influences on the dynamics of motion-induced blindness. *Journal of Vision*, *9*(1), 1–9. Doi: http://doi.org/10.1167/9.1.38

Shibata, M., Kawachi, Y., & Gyoba, J. (2010). Combined effects of perceptual grouping cues on object representation: Evidence from motion-induced blindness. *Attention, Perception & Psychophysics*, *72*(2), 387–397. Doi: http://doi.org/10.3758/APP

Shimojo, S. (2008). Self and world: large scale installations at science museums. *Spatial Vision*, *21*(3-5), 337–346. Doi: http://doi.org/10.1163/156856808784532536

Shinar, D., McDowell, E. D., & Rockwell, T. H. (1977). Eye Movements in Curve Negotiation. *Human Factors*, *19*(1), 63–71. Retrieved from http://hfs.sagepub.com/content/19/1/63.full.pdf

Skrandies, W. (1987). The upper and lower visual field of man. *Progress in Sensory Physiology*, *8*, 1–93. Retrieved from http://geb.uni-giessen.de/geb/volltexte/2009/7087/pdf/Skrandies_UpperLower_1987.pdf

Tabachnick, B. G. & Fidell, L. S. (2013). *Using Multivariate Statistics* (6th ed.). New Jersey: Pearson Education Inc.

The F-35 Helmet. (n.d.). Retrieved October 1, 2005 from https://www.f35.com/about/capabilities/helmet

Underwood, G., Crundall, D. E., & Chapman, P. R. (1997). Visual attention while performing driving and driving-related tasks. *Behavioural Research in Road Safety*, *7*, 60–73. Retrieved from https://trid.trb.org/view.aspx?id=635153

U.S. Department of Transportation. (1994). *Lane Change/Merge Crashes: Problem Size Assessment and Statistical Description.* Retrieved from http://ntl.bts.gov/lib/jpodocs/repts_te/420.pdf

Wallis, T. S. A., & Arnold, D. H. (2008). Motion-induced blindness is not tuned to retinal speed. *Journal of Vision, 8*(2), 1-7. Doi: 10.1167/8.2.11

Wallis, T. S. A., & Arnold, D. H. (2009). Motion-Induced Blindness and Motion Streak Suppression. *Current Biology*, *19*(4), 325–329. Doi: http://doi.org/10.1016/j.cub.2008.12.053

Wang, S., Fukuchi, M., Koch, C., & Tsuchiya, N. (2012). Spatial Attention Is Attracted in a Sustained Fashion toward Singular Points in the Optic Flow. *PLoS One, 7*(8), 1-13. Doi: 10.1371/journal.pone.0041040

Wells, E. T., & Leber, A. B. (2014). Motion-induced blindness is influenced by global properties of the moving mask. *Visual Cognition*, *22*(1), 125–140. Doi: http://doi.org/10.1080/13506285.2013.875500

Wells, E. T., Leber, A. B., & Sparrow, J. E. (2011). The role of mask coherence in motion-induced blindness. *Perception*, *40*(12), 1503–1518. Doi: http://doi.org/10.1068/p6976